Source mechanism of the July 13, 2002 Earthquake Kingri, Balochistan

TARIQ MAHMOOD & MOHAMMAD QAISAR
Micro Seismic Study Programme, Dr. Ishfaq Ahmad Research Laboratories
P.O. Nilore, Islamabad, Pakistan

ABSTRACT: *Teleseismic body waves recorded at worldwide 12 digital seismic stations were used to study the source process of the July 13, 2002 earthquake that occurred near Kingri, Balochistan. The P and SH waveforms of this event recorded by IRIS Digital Global Seismographic Network were inverted to double couple source using the method of Kikuchi and Kanamori (1986). The azimuthal coverage of seismograph stations is good enough to resolve some details of heterogeneous moment tensor. The focal mechanism solution shows strike slip faulting having strike 144.6°, dip 31.5°, and rake -7°. The seismic moment is estimated as 3.2 x 10^{17} Nm. The solution of the event is compared with fault plane solution derived from first motion polarity data recorded by local seismic network and also with the Harvard CMT solution. The moment tensor solution is in agreement with those obtained from first motion polarity and CMT solution.*

INTRODUCTION

On July 13, 2002 a moderate earthquake of magnitude $M_b = 5.8$ occurred near Kingri, a small town in Balochistan, about 100 km NW of Dera Ghazi Khan (Fig. 1). The region is mountaineous and sparsely populated. The earthquake occurred at 30.64°N and 69.86°E within the Kirthar-Sulaiman Shear zone having a moment magnitude of $M_w = 5.7$ was followed by 22 aftershocks of magnitude $\geq$2.0 within 48 hours up to July 15, 2002. Hypocenter locations of the aftershocks were determined with the help of computer code HYPO71PC (Lee, 1990) using body waves data recorded by local seismic network. The spatial distribution of the well-located aftershocks forms a cluster south of the main shock (Fig. 2).

The main purpose of this study is to determine the mechanism of this event including fault geometry, fault area, seismic moment and other related source parameters, using waveform inversion. Determination of these parameters is useful not only for understanding the physics of earthquakes but also for estimating the potential hazard associated with stress changes in the faults adjacent to the earthquake area.

SEISMOTECTONICS OF THE REGION

The area under study lies in the eastern part of Sulaiman arc in a belt of east-west trending arcurate and convex to the south thrust and fold. The mountains in the region form arcuate, parallel to sub parallel and en-echelon ranges of a few tens of kilometers to over 300 km long. The north-west trending left-lateral wrench Kingri fault lies within the Sulaiman seismic zone that covers the entire Sulaiman fold–thrust belt and is characterized by shallow earthquakes of moderate to high magnitude (Kazmi and Jan, 1997). This belt is bonded by Khalifat fault in the north, Tatra fault in the south and

Geological control on natural hazards: earthquakes and mass movement. Khan, M.A., Abbasi, I.A., & Khattak, G.A. (Eds.). Geological Bulletin, University of Peshawar, (Special Issue), Vol. 35, pp. 57–65, 2002

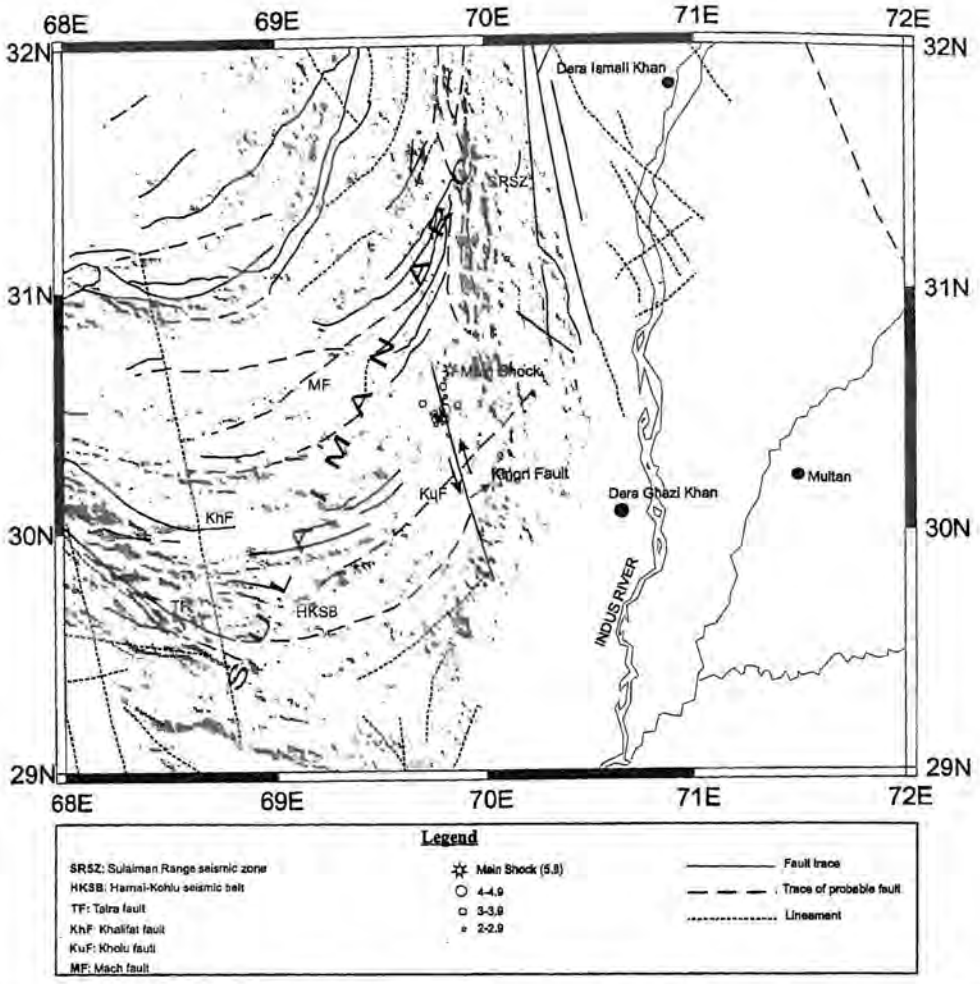

Fig.1 Seismotectonic map of Sulaiman arc and surrounding regions (from Kazmi and Jan, 1997) location of main shock (star), after shock (open circle) and Kingri fault.

Kingri fault in the east (Fig. 1). It is traversed by a number of large north-east, east-west and north-west trending faults. The seismicity in this region is supposed to be the result of movement on single, continuous fault or else it may be due to activity on a number of smaller but similar oriented faults (Quittmeyer et al., 1979).

DATA

The teleseismic broadband data set used in this study was retrieved from Data Management Centre of the Incorporated Research Institute of Seismology (IRIS-DMC) in the epicentral distance ranges between 30° and 90°. In this distance range, the waveforms are not contaminated by strong upper mantle or core phases. Fifteen body wave records from 11 stations, including vertical P and horizontal SH components, were used in this study to derive the source process of this earthquake. Stations parameters are given in Table 1 and displacement records of P waves as well as SH waves are shown in Fig. 3.

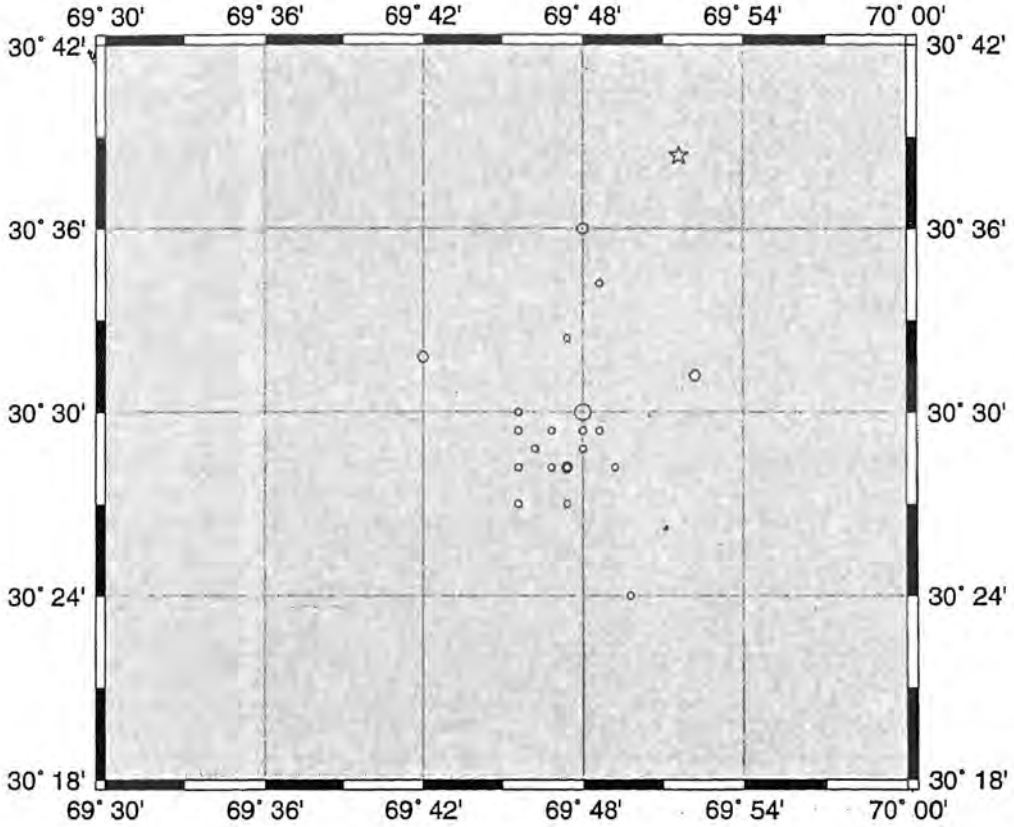

Fig.2 Epicenter of mainshock and its aftershocks according to the size of magnitude. Star indicates the location of main shock.

Using IASPEI (1991) Seismological travel time-tables, the teleseismic body waves data were windowed for one minute starting 10 s before P-wave arrival or S-wave arrival. The information contained in this time window is adequate to resolve the source process. The azimuthal coverage is good enough to resolve some details of the moment release distribution (Fig. 4-5).

TELESEISMIC BODY WAVE INVERSION

We employed an iterative deconvolution inversion method developed by Kikuchi and Kanamori (1986 and 1991) for teleseismic data to resolve the source complexity by matching the waveforms and extraction of the source parameters. First, with the approximations of a single point source, we determined the fault mechanism so that synthetic waveforms are best fit with the observed ones. For the synthetic waveform we used a three layer structures (Two layers of crust and a semi-infinite mantle) following the crustal model determined by (Qaisar et al., 1991) with only a minor modification in the source region as given in Table 2. The first step of inversion was the calculation of Green's function for the six element of the moment tensor at different depths beneath the epicenter, assuming a single point source. The focal depth lies within this depth range. In order to get a more realistic waveform, we have to consider the effects of inhomogenity in structure, attenuation during traveling and instru-

TABLE 1

LIST OF STATION PARAMETERS

Station	AZM	BK-AZM	Delta	P	1/r	Travel Time	Arrival Time (t1)	Start Time (t2)	$(t1-t2)_{JB}$ (Sec)
EILp	277.0	79.0	30.1	0.082	19.10	20:06:08	20:12:34	20:11:37	50
ULNp	48.0	-107.7	33.1	0.079	12.90	20:06:35	20:13:60	20:11:49	71
ULNs	48.0	-107.7	33.1	0.137	12.90	20:11:54	20:18:20	20:08:47	573
BJTp	62.9	-89.2	38.5	0.075	9.80	20:07:26	20:13:52	20:11:54	118
HIAp	48.7	-97.6	41.7	0.074	9.30	20:07:47	20:14:13	20:12:45	88
GRFOp	311.2	90.0	47.3	0.071	8.60	20:08:34	20:15:00	20:14:00	60
MDJp	55.6	-85.5	48.2	0.070	8.50	20:08:40	20:15:06	20:13:45	81
MBARp	237.4	46.4	48.5	0.070	8.40	20:08:41	20:15:07	20:14:02	65
BFOp	309.5	87.5	49.2	0.070	8.50	20:08:47	20:15:14	20:14:09	65
YAKp	32.4	-100.9	49.2	0.070	8.40	20:08:47	20:15:14	20:13:57	77
YAKs	32.4	-100.9	49.2	0.121	8.40	20:15:53	20:22:19	20:08:50	535
TIXIp	20.2	-109.4	51.5	0.068	8.20	20:09:05	20:15:31	20:13:58	93
TIXIs	20.2	-109.4	51.5	0.118	8.20	20:16:25	20:22:51	20:11:46	723
PETp	41.5	-71.2	65.3	0.058	6.90	20:10:43	20:17:09	20:15:51	78
PETs	41.5	-71.2	65.3	0.100	6.90	20:19:28	20:25:54	20:12:50	830

BK. AZM = Azimuth from station to source, P = Ray Parameter (P=Sin i/v where i=angle of incidence)
1/r = Geometrical factor (x1/10 km), $(t_1 - t_2)_{JB}$ = Time from Jeffrey Bullen Table

ments response. For Q attenuation a Futterman (1962) operator t* (ratio of travel time to average Q) of 1s was used for P waves and 4s for S waves (Helmberger, 1983). This Q filter was convolved with a triangular source time function having rise time τ_1 of 2s, source duration τ_2 of 8s and the seismic moment ~ 10^{18} Nm. Consequently the seismograms were simultaneously inverted to double couple single point source in the least square sense for the source model parameter, assuming no change in the mechanism during rupture. The inversion process was carried over different depths. The depth yielding the minimum residual was taken as the depth of the source.

For this event a point source model provides more or less equal fits to most of the waveforms. This means that a single source is sufficient to describe the source process of this earthquake. The P wave records as well as the SH waves, at different stations (Fig. 3) also reflect a smooth rupture. The fit of data i.e. synthetic and observed waveforms for the point

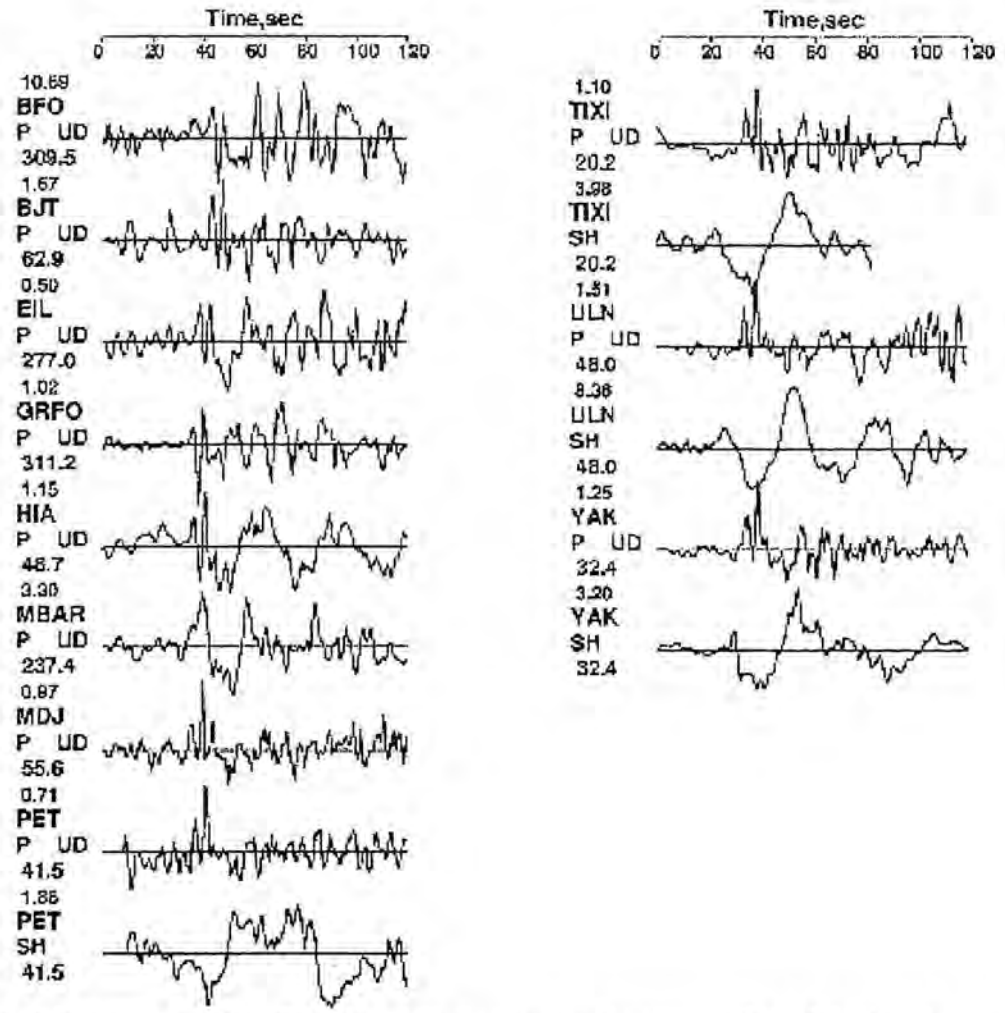

Fig. 3 Body waves recorded by IRIS stations used in the present waveform inversion for the Balochistan Earthquake of July 13, 2002.

TABLE 2

NEAR SOURCE STRUCTURE USED IN THEWAVEFORM INVERSION

V_p	V_s	ρ	D
5.57	3.36	2.65	15
6.50	3.74	2.87	33
8.10	4.68	3.30	–

Where V_p, V_s = P-wave and S-wave velocities (km/s) ρ = density (10^3 kg/m^3); D = thickness (km)

source model is shown in Fig. 6a-c. The final residual waveform error is 0.5951. The best matching double couple has a strike of 144.6°, a dip of 31.5° and a rake of –7°, strike slip-faulting mechanism.

Moreover, inversion was done using this solution as a fixed mechanism with the result indicating a good fit to the data with a final residual error equal to 0.5951. A slight change in the parameters of the fault plane caused an increase in the residual error. The final parameters of this solution are summarized in Table 3.

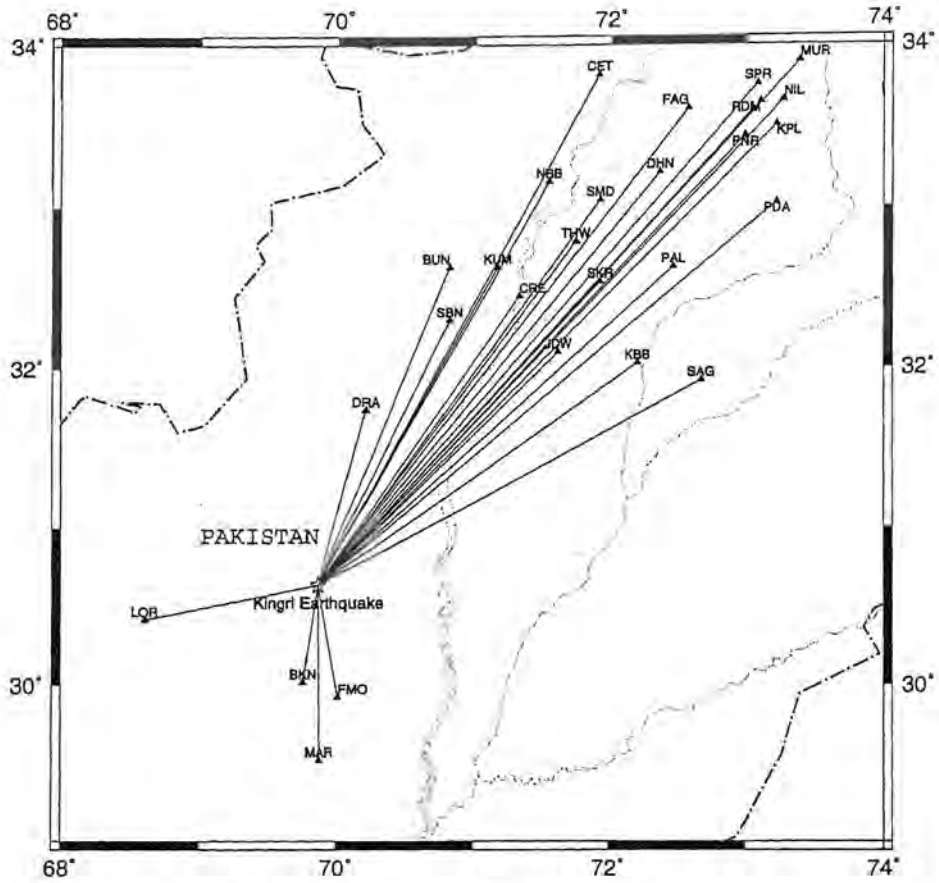

Fig. 4 Map of Kingri Earthquake and MSSP Seismic Network. Star denotes the Earthquake and solid triangles denote the seismic stations.

CALCULATION OF STRESS DROP AND DISLOCATION

Assuming the bilateral rupture propagation, the fault area of this event can be estimated using the relation of Fukao and Kikuchi (1987).

$$S = \pi (V\tau_2 / 2)^2$$

where V is the rupture velocity and τ represents the rupture duration. Rupture velocity is taken as V = 2.5 km/sec for shallow earthquakes. After estimating the aftershock area S, we obtained the average stress drop ($\Delta\sigma$) following Fukao and Kikuchi (1987) as

$$(\Delta\sigma) = 2.5\, M_o / S^{3/2}$$

TABLE 3

FINAL SOURCE PARAMETERS

Φ	δ	λ	H	M_o	M_w	$\Delta\sigma$	τ_1	τ_2
144.6	31.7	-7	23.0	3.2×10^{17}	5.7	4	2	8

Where Φ = Strike; δ = Dip; λ = Slip; M_o = Seismic Moment; M_w = Moment Magnitude; $\Delta\sigma$ = tress Drop; τ_1 = Rise Time; τ_2 = Source Duration

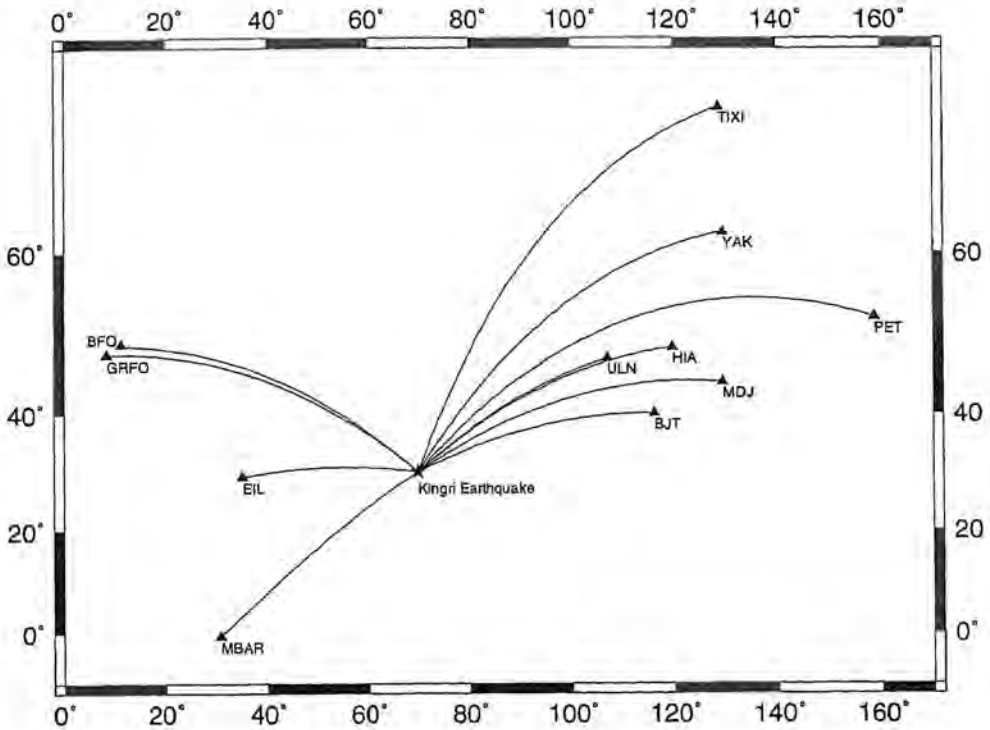

Fig. 5 IRIS broadband seismograph stations used in the present wave form inversion. Star denotes the main shock and solid triangles denote the IRIS stations.

where M_o is the seismic moment. The stress drop corresponding to this event is 4 bars. According to the slip dislocation theory of faulting (Aki, 1966) the average dislocation (D) can be estimated from

$$D = M_o / \mu S$$

where μ is the rigidity (3×10^{10} N/m^2). The displacement from the above relation is estimated as D = 0.53 m. The dislocation velocity can be determined from the dislocation-time history following Kanamori (1972)

$$D^o = D/\tau/2$$

The value obtained in this study is 0.03 m/s for a rise time of 2 s.

RESULTS AND DISCUSSIONS

The mechanism diagram for the total moment release is shown in Fig. 7. It is comparable with solutions obtained by Harvard University CMT and MSSP first motion polarity data. Our solution is well in agreement with other mentioned solutions. Fig 6(a) shows the moment rate function and its area that gives the total seismic moment $M_o = 3.2 \times 10^{17}$ Nm. A comparison between observed and the generated synthetic waveforms that matches satisfactorily well at all stations are shown in Fig. 6 (c).

Modeling of body waves recorded at teleseismic distances has shown that the fault causing this earthquake has a left lateral strike slip fault with a roughly NW-SE trend. As shown in Fig. 1, the epicenter of main shock and its aftershocks lie in a region, which is traversed by a number of NS-EW trending lineaments and a long prominent fault trending NW-SE. The fault trending NW-SE is supposed to be active with a left lateral strike slip movement. The location/orientation of epicenters of the main shock and its aftershocks suggest that the recent activity is associated with the fault trending

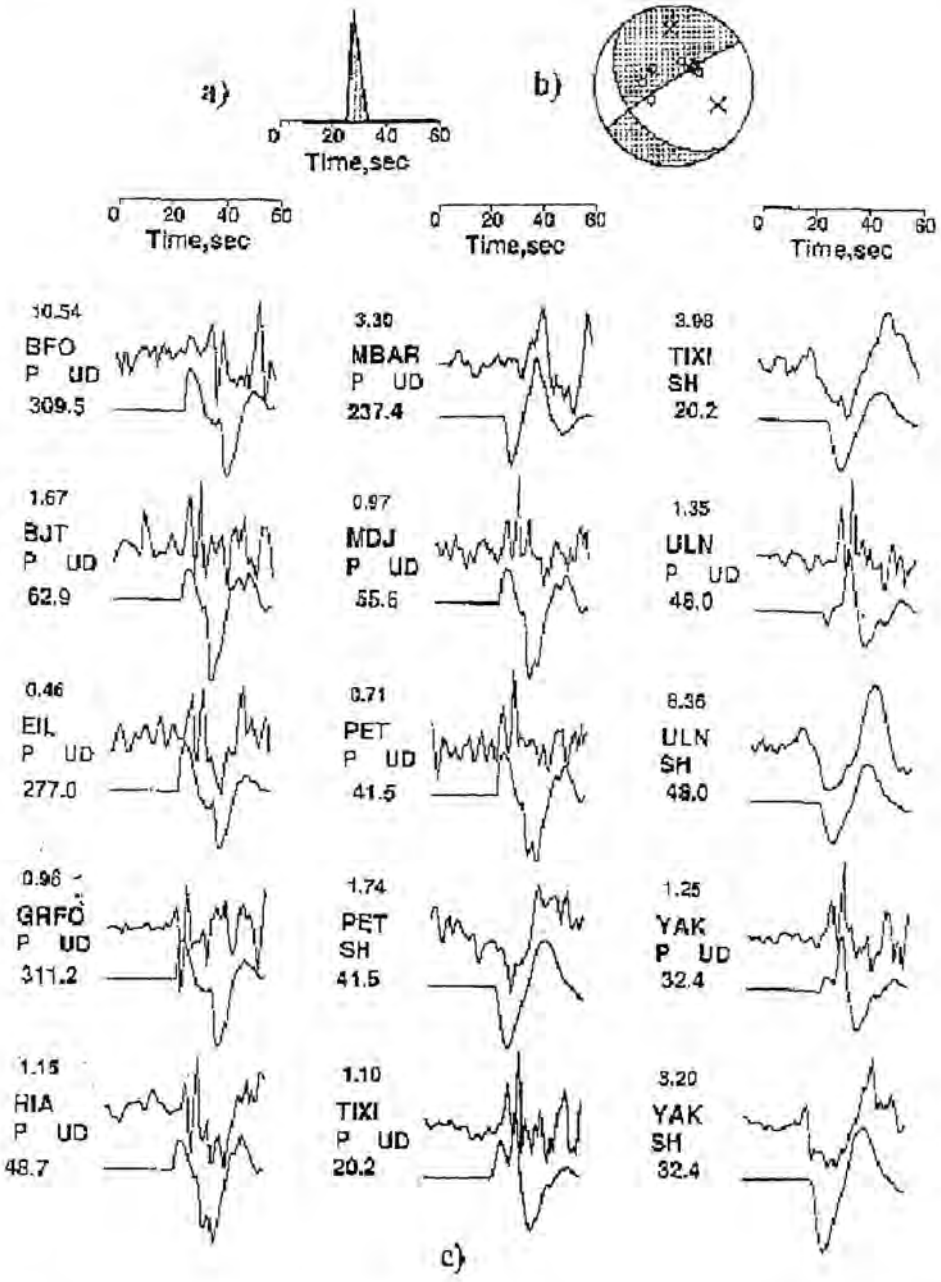

Fig. 6 Results of the inversion with a double couple source. A) Seismic moment release as a function of time b) mechanism diagram of the best fit double couple point source c) observed and synthetic P and SH waveforms. The numbers in the upper and lower left indicate peak to peak amplitude in microns of the observed records and the azimuth respectively.

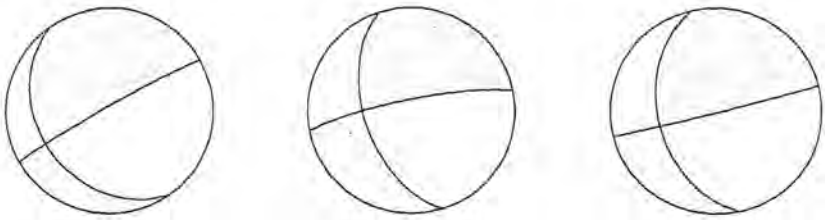

Fig. 7 Mechanism diagram of the total moment tensor. It is compared with the solution obtained by Harvard University and first motion polarity data at MSSP local seismic network. The seismic moment is given in units of 10^{17} Nm.

NW-SE i.e. the Kingri fault. This is further corroborated by the focal mechanism solution of this earthquake obtained from first motion polarity data that also shows a left lateral strike slip movement on the NW-SE trending plane. This earthquake had a shallow crustal focal depth of 23 km. The cluster of aftershocks indicates nearly the same fault length with unilateral southward rupture propagation. The seismic moment released along the fault is 3.2×10^{17} Nm. This seismic moment correspond to a moment magnitude of 5.7. The stress drop associated with a fault area of 200 km^2 is equal to 4 bars.

Acknowledgements: The authors are thankful to Mr. Karam Khan, Mr. Zahid Ali and Mr. Mohammad Ali Shah for assisting with various aspects of this study and also to Mr. Abdul Hakim for constructive comments on the manuscripts.

REFERENCES

Aki, K. 1966. Generation and propagation of G waves from the Niigata earthquake at June 16, 1964. Bull. Earthquake Res. Inst., Tokyo Univ., 44, 73-88.

Fukao, Y. & Kikuchi, M. 1987. Source retrieval for mantle earthquakes by iterative deconvolution of long period P-waves. Tectonophysics, 144, 249-269.

Futterman, W.I. 1962. Dispersive body wave. Journal of Geophysics. Res., 67, 5279-5291.

Helmberger, D.V. 1983. Theory and application of synthetic seismograms, in Earthquakes, Observation, Theory and Interpretation (Societa Italiana di Fisica, Bologna, Italy), 174-222.

Kanamori, H. 1972. Determination of effective tectonic stress associated with earthquake faulting: the Tottori earthquake of 1943. Phys. Earth Planet Interior., 5, 426-434.

Kazmi, A. H. & Jan, M. Q. 1997. Geology and Tectonics of Pakistan. Graphic Publishers, Nazimabad, Karachi. 410-413.

Kennett, B. L. N. 1991. IASPEI 1991 Seismological Tables. Research School of Earth Sciences, Australian National University, Canberra ACT 2601, Australia.

Kikuchi, M. & Kanamori, H. 1986. Inversion of complex body waves –II. Phys. Earth Planet Interior., 43, 205-222.

Kikuchi, M. & Kanamori, H. 1991. Inversion of complex body waves –III. Bull. Seismol. Soc. Am., 79, 670-689.

Lee, W.H.K. 1990. HYPO71PC Programme. IASPEI Software Library, Vol. 1.

Qaisar, M., Shahid, M. B., Tariq, M. & Mubarak, M. A. 1991. Simultaneous inversion of velocity structure and hypocentral locations: Application to the area around the proposed Kalabagh Dam site, Pakistan. MSSP-41/91.

Quittmeyer, R. C., Farah, A. & Jacob, K. H. 1979. The Seismicity of Pakistan and the relation to surface faults. In: Farah, A. & Delong, K. A. (eds.) Geodynamics of Pakistan. Geol. Surv. Pak., Quetta, 351-358.